One Dimensional Viscous Shock Analysis

Department of Aerospace and Mechanical Engineering

University of Notre Dame
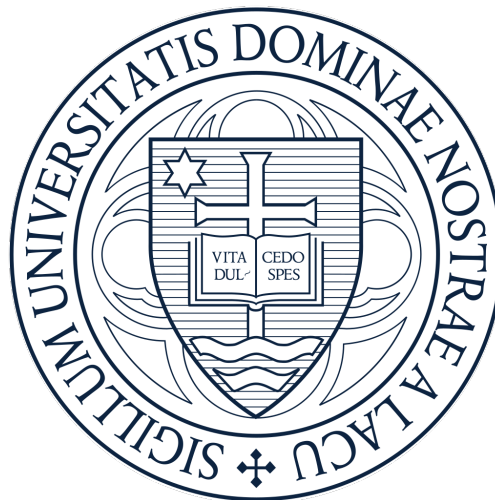
Prepared by: Gregory T. Golonka

Prepared for: AME 48491 - Undergraduate Research

Joseph M. Powers

Notre Dame, Indiana 46556

December 12, 2024

Abstract

The objective of this research is to predict the continuous structure of a shock wave. This structure is analyzed using the governing conservation equations from fluid dynamics in the steady wave reference frame. This paper will study the effects of non-reactive mixtures of helium molecules to evaluate the effect of mass diffusion across a shock. The helium model will act as the framework for a reactive model using Arrhenius kinetics to understand the effect of diatomic molecule dissociation across a shock wave. The study provides a numerical solution to the system of ordinary differential equations to determine the shock thickness. Ultimately, the study finds that a $M = 2.55$ shock through helium at ambient conditions $T = 300$ K and $\rho = 1.615$ kg/m^3 results in a shock thickness of 10^{-4} mm.

Contents

Nomenclature

$\hat{x}$	laboratory frame position - m	a	species a	
x	wave frame position - m	b	species b	
$\hat{t}$	laboratory frame time - s	Y_i	mass fraction	
t	wave frame time - s	j_i	mass diffusion flux- $\frac{\text{kg}}{\text{m}^2\,\text{s}}$	
$\hat{u}$	laboratory frame fluid velocity - $\frac{\text{m}}{\text{s}}$	M_i	molar mass - $\frac{\text{kg}}{\text{kmol}}$	
u	wave frame velocity - $\frac{\text{m}}{\text{s}}$	$\dot{\omega}_i$	molar production rate - $\frac{\text{kmol}}{\text{m}^3\,\text{s}}$	
U	wave speed - $\frac{\text{m}}{\text{s}}$	ν_{ij}	net stoichiometric coefficients	
$\overline{\rho}$	molar concentration - $\frac{\text{kmol}}{\text{m}^3}$	ν'_{ij}	stoichiometric coefficients of products	
ρ	density - $\frac{\text{kg}}{\text{m}^3}$	ν''_{ij}	stoichiometric coefficients of reactants	
T	temperature - K			
τ	viscous shear stress - Pa	r_j	reaction rate - $\frac{\text{kmol}}{\text{m}^3\,\text{s}}$	
p	pressure - Pa	k_j	Arrhenius rate -	
$\overline{e}$	internal energy - $\frac{\text{kJ}}{\text{kmol}}$		$\left(\frac{\text{kmol}}{\text{m}^3}\right)^{(1-\sum_{j=1}^{J}\nu'_j)}/\text{s}$	
e	internal energy - $\frac{\text{kJ}}{\text{kg}}$	a_j	collision frequency factor	
$\overline{h}$	enthalpy - $\frac{\text{kJ}}{\text{kmol}}$		$\left(\frac{\text{kmol}}{\text{m}^3}\right)^{(1-\sum_{j=1}^{J}\nu'_j)}/\text{s}\,/\,\text{K}^{\beta}$	
h	enthalpy - $\frac{\text{kJ}}{\text{kg}}$	β_j	temperature dependency exponent	
q	heat flux - $\frac{\text{W}}{\text{m}^2}$			
k	thermal conductivity - $\frac{\text{W}}{\text{m K}}$	$\overline{\mathcal{E}}_j$	activation energy - $\frac{\text{kJ}}{\text{kmol}}$	
Pr	Prandtl number	$K_{c,j}$	equilibrium constant -	
α	thermal diffusivity - $\frac{\text{m}^2}{\text{s}}$		$\left(\frac{\text{kmol}}{\text{m}^3}\right)^{\left(\sum_{i=1}^{N}\nu'_i-\sum_{i=1}^{N}\nu''_j\right)}$	
$\mathcal{D}$	mass diffusivity - $\frac{\text{m}^2}{\text{s}}$	G_j^0	Gibbs free energy - $\frac{\text{kJ}}{\text{kmol}}$	
ν	kinematic viscosity - $\frac{\text{m}^2}{\text{s}}$	c_p	constant pressure specific heat - $\frac{\text{kJ}}{\text{kg K}}$	
$\overline{R}$	universal gas constant - $\frac{\text{kJ}}{\text{kmol K}}$			
μ	dynamic viscosity - Pa s	c_v	constant volume specific heat - $\frac{\text{kJ}}{\text{kg K}}$	
i	species index			
j	reaction index	γ	ratio of specific heats	
N	number of species	λ	mean free path - m	
J	number of reactions			

1 Introduction

This study aims to advance the understanding of shock wave structure and its interaction with reactive systems. Shock waves have applications in fields such as propulsion, detonation physics, and high-speed flow analysis; therefore, a simplified example is explored to take a tentative step toward future goals. The ultimate purpose is to analyze the dissociation of diatomic molecules across a viscous shock structure. The dissociation of molecules is important across the shock structure because it is the reaction process that occurs when extreme temperatures cause molecular bonds to break. Understanding how these bonds respond within a shock wave is important as technology advances.

1.1 Research Objectives

For this paper, a simplified model will be studied utilizing an inert gas, helium, separated into two separate species, species a and species b. Both species share the same fluid properties such as density, temperature, velocity, specific heat, specific gas constant thermal conductivity, and dynamic viscosity. However, splitting the inert gas into two species allows for an analysis of the structure and mass diffusion across the shockwave.

The study will examine a left-moving wave with a speed of 1226.017 m/s and will be analyzed in the wave reference frame. The wave speed can be visualized between the laboratory frame and the shock frames in Figure 1.
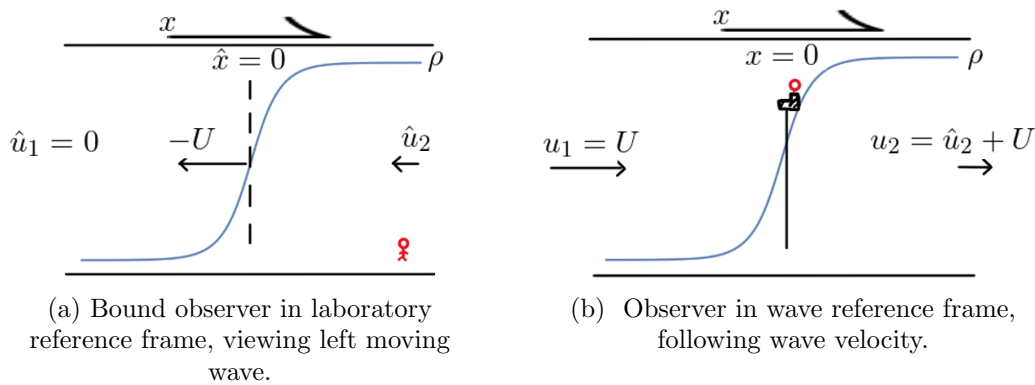

(a) Bound observer in laboratory reference frame, viewing left moving wave.

(b) Observer in wave reference frame, following wave velocity.

Figure 1: Fluid velocities in different reference frames

Figure 1 shows the pre and post-shock velocities $\hat{u}_1$ and $\hat{u}_2$ in the laboratory reference frame: meaning a fixed observer watches the shock move from right to left. Whereas, u_1 and u_2 are the unshocked and shocked fluid velocities in the wave reference frame: meaning the observer travels with the shock. Furthermore, Figure 1 shows the transformations between the two reference frames, with the respective directional changes. Furthermore, the shock thickness is shown across the density profile, where ρ is the shock density.

The Navier-Stokes equations will be used to exhibit the internal structure of a shock wave. To solve the differential equations, a steady-state assumption was made. After assuming a steady state, the conservation equations were manipulated into one ordinary differential equation with one variable. Then, utilizing the pre-shock state as a boundary condition, the differential equation could be solved to model the structure of the shock. Once one property was solved, the others could be calculated by substituting into the original conservation equations. The mixture models are also used to calculate the mass diffusion and reaction properties of a shock wave.

In this study an inert mode will be used, forcing the species molar production rate to zero, meaning there is no reaction in the system. The system of differential equations will first be analyzed in a phase plane, giving the boundary conditions. After utilizing the phase plane, the system can be further simplified to solve using first-order methods.

1.2   Literature Review

Here we review the literature of viscous shock waves. There are both theoretical and experimental studies that outline the structure of a shock wave. Using these studies we can build our model.

Early theoretical studies on the structure of shock waves were conducted by researchers such as Vincenti and Kruger [1], Liepmann and Roshko [2], and Zeldovich [3]. While each of these works addresses a slightly different aspect of the problem, they are all grounded in the same fundamental principle: the shock structure must satisfy the Navier-Stokes equations

at all points within its domain.

Vincenti and Kruger computed a model to analyze a shock structure of a right moving wave at $M = 1.7$. Their chosen medium was a non-inert gas argon, such that they could discover how close their results matched with the experimental results of Talbot and Sherman from 1959 [4]. Ultimately discovering that the their theoretical results match the experimental.

Thompson [5] also outlines the importance of the shock structure. The inviscid, assumption presupposes that the velocity and temperature gradients are infinite at the shock front, inducing infinite viscous stress and heat flux from the shock. To avoid the infinite viscous stress and heat flux, the extended *shock layer* reduces the velocity and temperature gradients. The internal shock layer is comparable to a boundary layer; in that both regions are characterized by large viscous stress and high heat flux bounded by external regions considered inviscid.

Liepmann and Roshko offer a more nuanced distinction between the two, and enforce the importance of the shock structure. The essential difference between the shock wave and the boundary layer lies in particle behavior. When a streamline enters a shock wave, it emerges downstream. Whereas when a streamline enters a boundary layer, it remains in a region of shear. Therefore, flowing through a shock wave, the particle transforms from one thermodynamic state to another. This distinction is widely accepted and mirrors the analyses found in [6, 7].

Zel'dovich expands this analysis of a shock wave structure into molecular reactions. Eventually analyzing the molecular dissociation and ionization of diatomic molecules across these waves. This research will set out the groundwork of the mathematical foundation of the work done by Zel'dovich. Meaning this paper will dive into a simplified version of Zel'dovich's problem, with no reaction.

Further experimental data show the existence of a viscous shock layer. In a study conducted by Sherman [8] to determine shock wave structures and relaxation periods, he found

the experimental data followed the Navier-Stokes approximations while including losses due to viscosity and heat. Sherman's experiment utilized a shock holder, a type of shock-producing device that consists of a thin-walled circular cylinder or cone frustum immersed into the uniform portion of a wind tunnel jet. Using this apparatus with the addition of temperature-sensitive resistance wires connected to a thermocouple, the system could analyze the temperature distribution across a shock. Figure 2 shows the dimensionless wire temperature, t_w, along the dimensionless wind tunnel length, y.
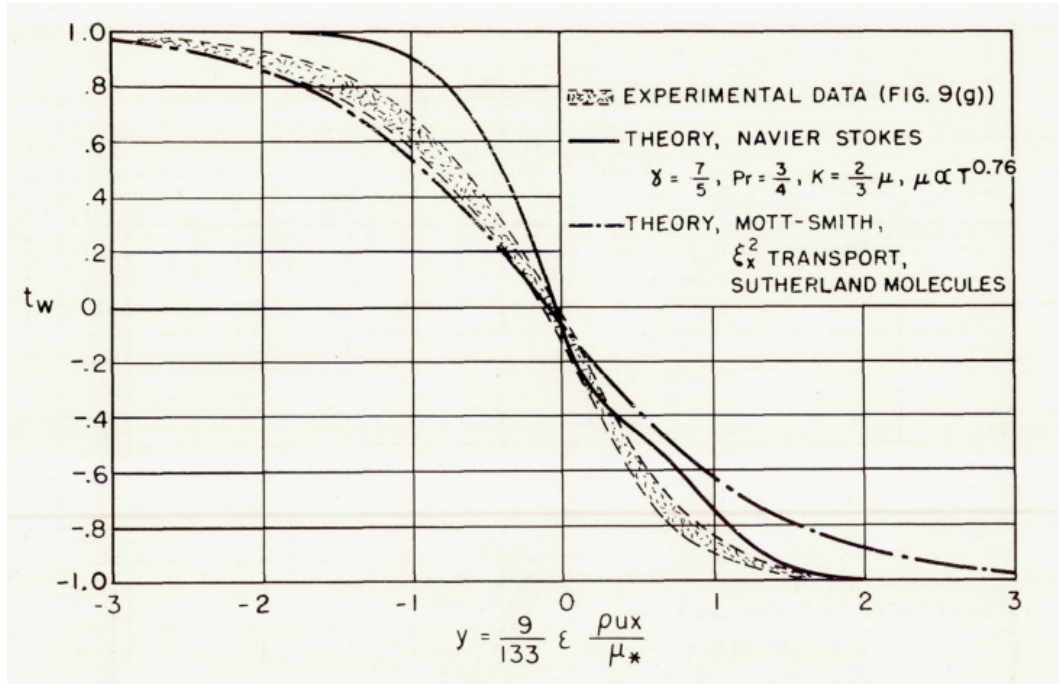

Figure 2: Comparison of various theories for a monotomic gas (helium). $M = 1.61$, Sherman [8].

2 Governing Equations

2.1 Mixture Model

To analyze the reactions occurring within a shock wave, a mixture model must be established. The Dalton model [9] is used. We will adopt the following rules for mixture properties:

$$p = \sum_{i=1}^{2} p_i, \quad 1 = \sum_{i=1}^{2} Y_i, \quad \rho = \sum_{i=1}^{2} \rho_i = \sum_{i=1}^{2} \frac{\overline{\rho_i}}{M_i}, \quad e = \sum_{i=1}^{2} Y_i e_i, \tag{1}$$

$$0 = \sum_{i=1}^{2} j_i, \quad h = \sum_{i=1}^{2} Y_i h_i, \quad c_p = \sum_{i=1}^{2} Y_i c_{pi}, \quad c_v = \sum_{i=1}^{2} Y_i c_{vi}, \tag{2}$$

$$T = T_i. \qquad V = V_i \tag{3}$$

The subscript i indicates that the property is a specific species property rather than the whole mixture. Here p is mixture pressure, Y_i is the species mass fraction, M_i is the molecular mass, e is the mixture internal energy h is the enthalpy, c_p is the mixture specific heat at constant pressure and c_v is the mixture specific heat at constant volume. Furthermore, p_i, ρ_i, $\overline{\rho_i}$, e_i, h_i, c_{pi}, c_{vi}, T_i, and V_i are species pressure, density, molar concentration, internal energy, enthalpy, constant pressure specific heat, constant volume specific heat, temperature, and volume.

2.2 Unsteady Conservative Form

The first step in analyzing the system is presenting the conservation equations and their different forms. The forms of all governing equations are standard and can be obtained from [10, 11, 1]. To express the conservation of mass, linear momentum, and energy in

conservative form and in the laboratory reference frame they are written as follows:

$$\frac{\partial \rho}{\partial \hat{t}} + \frac{\partial}{\partial \hat{x}} (\rho \hat{u}) = 0, \tag{4}$$

$$\frac{\partial}{\partial \hat{t}} (\rho \hat{u}) + \frac{\partial}{\partial \hat{x}} \left(\rho \hat{u}^2 \right) + \frac{\partial}{\partial \hat{x}} (p - \tau) = 0, \tag{5}$$

$$\frac{\partial}{\partial \hat{t}} \left(\rho \left(e + \frac{\hat{u}^2}{2} \right) \right) + \frac{\partial}{\partial \hat{x}} \left(\rho \hat{u} \left(e + \frac{\hat{u}^2}{2} + \frac{p}{\rho} \right) + (\tau \hat{u} - q) \right) = 0. \tag{6}$$

Here, $\hat{x}$, $\hat{t}$ and $\hat{u}$ represent the position, time, and velocity of a particle in the laboratory reference frame. The variable q denotes the heat flux, while τ represents the shear stress. These forms are conservative because the quantities that are conserved are within the time derivative; i.e. mass, linear momenta, and energy.

The evolution of chemical species is given by,

$$\frac{\partial}{\partial \hat{t}} (\rho Y_i) + \frac{\partial}{\partial \hat{x}} (\rho Y_i \hat{u} + j_i) = M_i \dot{\omega}_i. \tag{7}$$

Here j_i is the mass diffusion flux of species i, and $\dot{\omega}_i$ is the species molar production rate. The species molar production rate $\dot{\omega}_i$ can be further expanded as,

$$\dot{\omega}_i = \sum_{j=1}^{2} \nu_{ij} r_j. \tag{8}$$

Here r_j is given by the law of mass action, and ν_{ij} is the stoichiometric coefficient for each species, per reaction. The law of mass action is then expanded as,

$$r_j = k_j \prod_{i=1}^{2} \overline{\rho}_i^{\nu'_{ij}} \left(1 - \frac{1}{K_{c,j}} \prod_{i=1}^{2} \overline{\rho}_i^{\nu_{ij}} \right). \tag{9}$$

The reaction rate, k_j, given by the Arrhenius kinetics rule, $\overline{\rho}$ is the molar concentration and $K_{c,j}$ is the equilibrium constant.

$$k_j = a_j T^{\beta_j} \exp \left(\frac{-\overline{\mathcal{E}}_j}{\overline{R} T} \right). \tag{10}$$

Here a_j is the collision frequency factor, β is a dimensionless parameter whose value is set by experiments, and $\overline{\mathcal{E}}_j$ is the activation energy needed for the reaction to occur. The equilibrium constant $K_{c,j}$ is defined as

$$K_{c,j} = \left(\frac{p_0}{\overline{R}T}\right)^{\sum_{i=1}^{2}\nu_{ij}} \exp\left(\frac{-\Delta G_j^0}{\overline{R}T}\right). \tag{11}$$

The reference pressure is defined as p_0, and $-\Delta G_j^0$ is the standard change in Gibbs free energy across the reactions. Expanding the heat flux, mass diffusion, and viscous shear stress as seen in Eq. (5) and Eq. (6), one obtains:

$$q = -k\frac{\partial T}{\partial \hat{x}} + \sum_{i=1}^{2} j_i h_i, \qquad j_i = -\rho\mathcal{D}\frac{\partial Y_i}{\partial \hat{x}}, \qquad \tau = \frac{4}{3}\mu\frac{\partial \hat{u}}{\partial \hat{x}}. \tag{12}$$

The thermal conductivity of the fluid particle is k. Additionally, $\mathcal{D}$ is the mass diffusivity and μ is the dynamic viscosity. The thermal equation of state is defined using the mixture models in combination with the ideal gas law.

$$p_i = \overline{\rho}_i\overline{R}T = \rho\overline{R}T\frac{Y_i}{M_i} = \overline{R}T\frac{\rho_i}{M_i} = \rho_i R_i T. \tag{13}$$

Therefore the mixture pressure is:

$$p = \overline{R}T\sum_{i=1}^{2}\overline{\rho}_i = \overline{R}T\sum_{i=1}^{2}\frac{\rho Y_i}{M_i} = \overline{R}T\sum_{i=1}^{2}\frac{\rho_i}{M_i}. \tag{14}$$

Here $\overline{R}$ is the universal gas constant.

2.3 Unsteady Non-Conservative Form

The conservative equations can be transformed into their non-conservative counterparts by simple calculus. Using the product rule to expand, the mass, linear momenta, energy, and species reaction equations can be simplified into the following:

$$\frac{\partial \rho}{\partial \hat{t}} + \hat{u}\frac{\partial \rho}{\partial \hat{x}} + \rho\frac{\partial \hat{u}}{\partial \hat{x}} = 0, \tag{15}$$

$$\rho\frac{\partial \hat{u}}{\partial \hat{t}} + \rho\hat{u}\frac{\partial \hat{u}}{\partial \hat{x}} + \frac{\partial}{\partial \hat{x}}(p - \tau) = 0, \tag{16}$$

$$\rho\left(\frac{\partial e}{\partial \hat{t}} + \hat{u}\frac{\partial e}{\partial \hat{x}}\right) + \frac{\partial q}{\partial \hat{x}} + \frac{\partial \hat{u}}{\partial \hat{x}}(p - \tau) = 0, \tag{17}$$

$$\rho\frac{\partial Y_i}{\partial \hat{t}} + \rho\hat{u}\frac{\partial Y_i}{\partial \hat{x}} + \frac{\partial j_i}{\partial \hat{x}} = M_i\dot{\omega}_i. \tag{18}$$

2.4   Galilean Transformation

The wave reference frame is chosen for the analysis of the inert helium because it simplifies the analysis making it easier to calculate changes in thermodynamic properties. To convert the laboratory reference frame to the steady wave frame, Galilean transformations are used:

$$x = \hat{x} + U\hat{t}, \qquad t = \hat{t}. \tag{19}$$

Here x and t are the position and time within the wave reference frame, while $\hat{x}$ and $\hat{t}$ are the position and time in the laboratory reference frame. In this study, the wave moves to the left, therefore the distance traveled by the shock $U\hat{t}$ is added to the lab frame position to get into the wave reference frame. The position of the shock at $x = 0$ within the wave frame. Using the transformation in Eq. (19), we find how the derivatives are represented under the coordinate transformation.

$$dx = \frac{\partial x}{\partial \hat{x}}\ d\hat{x} + \frac{\partial x}{\partial \hat{t}}\ d\hat{t} = d\hat{x} + U\ d\hat{t}, \tag{20}$$

$$dt = \frac{\partial t}{\partial \hat{x}}\ d\hat{x} + \frac{\partial t}{\partial \hat{t}}\ d\hat{t} = d\hat{t}. \tag{21}$$

By scaling dx by dt, we can derive the transformation for the velocities.

$$\frac{dx}{dt} = \frac{d\hat{x}}{d\hat{t}} + U, \tag{22}$$

$$u = \hat{u} + U. \tag{23}$$

Here we are taking the particle velocity in the wave frame $u = dx/dt$ and the particle velocity in the laboratory frame as $\hat{u} = d\hat{x}/d\hat{t}$. Furthermore, a generic dependent variable ψ can be defined such that it has a representation in the original space, $\psi(\hat{x}, \hat{t})$, and the transformed space, $\psi(x, t)$. These two points must map to the same space, such that:

$$\psi(\hat{x}, \hat{t}) = \psi(x, t). \tag{24}$$

Therefore the derivative of ψ can be expressed as the following:

$$d\psi = \left.\frac{\partial \psi}{\partial \hat{x}}\right|_{\hat{t}} d\hat{x} + \left.\frac{\partial \psi}{\partial \hat{t}}\right|_{\hat{x}} d\hat{t} = \left.\frac{\partial \psi}{\partial x}\right|_{t} dx + \left.\frac{\partial \psi}{\partial t}\right|_{x} dt. \tag{25}$$

Using the expressions of the wave frame derivatives found in Eq. (20) and Eq. (21), the expression can be simplified to:

$$d\psi = \left.\frac{\partial \psi}{\partial \hat{x}}\right|_{\hat{t}} d\hat{x} + \left.\frac{\partial \psi}{\partial \hat{t}}\right|_{\hat{x}} d\hat{t} = \left.\frac{\partial \psi}{\partial x}\right|_{t} dx + \left.\frac{\partial \psi}{\partial t}\right|_{x} dt, \tag{26}$$

$$= \left.\frac{\partial \psi}{\partial x}\right|_{t} (d\hat{x} + U \, d\hat{t}) + \left.\frac{\partial \psi}{\partial t}\right|_{x} d\hat{t}, \tag{27}$$

$$= \left.\frac{\partial \psi}{\partial x}\right|_{t} dx + \left(\left.\frac{\partial \psi}{\partial t}\right|_{x} + U \left.\frac{\partial \psi}{\partial x}\right|_{t}\right) d\hat{t}. \tag{28}$$

Now we consider Eq. (28) for constant $\hat{x}$, causing $d\hat{x} = 0$, and we divide by $d\hat{t}$.

$$\left.\frac{\partial \psi}{\partial \hat{t}}\right|_{\hat{x}} = \left.\frac{\partial \psi}{\partial t}\right|_{x} + U \left.\frac{\partial \psi}{\partial x}\right|_{t}. \tag{29}$$

Simplifying further the partial with respect to $\hat{t}$ becomes

$$\frac{\partial}{\partial \hat{t}}\bigg|_{\hat{x}} = \frac{\partial}{\partial t}\bigg|_{x} + U \frac{\partial}{\partial x}\bigg|_{t}. \tag{30}$$

Furthermore, to analyze the steady state solution of a reaction, for constant t, $dt = 0$, therefore Eq. (28) reduces to:

$$\frac{\partial}{\partial \hat{x}}\bigg|_{\hat{t}} = \frac{\partial}{\partial x}\bigg|_{t}. \tag{31}$$

Eq. (31) is ultimately the transformation that can be used to redefine the governing equations from the laboratory frame to the wave reference frame. The result is invariant, meaning changing between the reference frames does not change the governing equations.

2.5 Steady Conservative Form

To convert the governing equations from unsteady to steady, time must remain constant. Therefore, all partial derivatives with respect to the independent variable t go to 0. Furthermore, all partial derivatives with respect to x become total derivatives, as described:

$$\frac{d}{dx}(\rho u) = 0, \tag{32}$$

$$\frac{d}{dx}\left(\rho u^2 + p - \tau\right) = 0, \tag{33}$$

$$\frac{d}{dx}\left(\rho u \left(e + \frac{u^2}{2} + \frac{p}{\rho}\right) + \tau u - q\right) = 0, \tag{34}$$

$$\frac{d}{dx}\left(\rho Y_i u + j_i\right) = M_i \dot{\omega}_i. \tag{35}$$

2.6 Steady Non-Conservative Form

Similarly to *steady conservative* forms of the governing equations, to transform the *unsteady non-conservative* governing equations into their steady counterparts, the time is taken to be

13

constant. The system can therefore be written as,

$$u\frac{d\rho}{dx} + \rho\frac{du}{dx} = 0, \tag{36}$$

$$\rho u\frac{du}{dx} + \frac{d}{dx}(p-\tau) = 0, \tag{37}$$

$$\rho u\frac{de}{dx} + \frac{dq}{dx} + \frac{du}{dx}(p-\tau) = 0, \tag{38}$$

$$\rho u\frac{dY_i}{dx} + \frac{dj_i}{dx} = M_i\dot{\omega}_i. \tag{39}$$

3 Inert Shock Wave Structure

The inert gas is used to stop all reactions in the study. Which in turn, further simplifies the conservation equations in combination with the steady-state assumption. With these assumptions, the steady wave structure and mass diffusion flux are calculated.

3.1 Boundary Conditions

The necessary boundary conditions need to be established to analyze the shock properties, such as velocity temperature, and density. The boundary conditions will be defined using the wave frame boundary conditions. Therefore, the boundary conditions in the wave frame can be defined as the post-shock state through the following parameters in Table 1

Table 1: Boundary conditions of shock properties

Property	Variable	Value	Units
velocity	u_1	1226.017	m/s
density	ρ_1	1.615	kg/m^3
temperature	T_1	209.44	K

Figure 3 shows the relationship that the density of the fluid experiences across a shock.
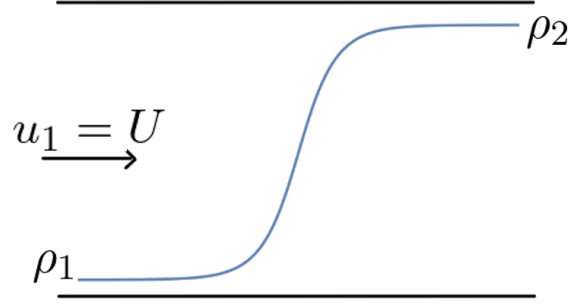
Figure 3: Sketch of steady wave structure for density

In Figure 3, ρ is the mixture density across the boundary. This study will only look into the steady-state solution across the applied x limits which simplifies the governing equations into one-dimensional ordinary differential equations.

3.2 Parameters

An inert gas is can be used to study the mass diffusion across the shock structure. Helium was chosen because it is the simplest gas for this model. The thermodynamic properties of helium can be found in Table 2 below:

Table 2: Properties of the helium at post-shock boundary condition [9]

Variable	Value	Units
c_v	3.116	kJ/kg/K
c_p	5.1931	kJ/kg/K
R	2.0771	kJ/kg/K
γ	5/3	
μ	3.674×10^{-7}	Pa s
k	0.002544	W/m/K
α	3.033×10^{-6}	m^2/s

In Table 2, the values below the dotted line represent the calculated properties given the assumption that the Prandtl number, Pr $= 3/4$.

3.3 Inert Shock Computations

For the simplified limits, the reaction rate, $\dot{\omega}$, equals zero and the species properties are taken to be the same. The shock takes place under steady-state conditions, and the governing equations for the viscous shock with diffusion and no reaction are as follows.

$$\frac{d}{dx}(\rho u) = 0, \tag{40}$$

$$\rho u \frac{du}{dx} + \frac{d}{dx}(p - \tau) = 0, \tag{41}$$

$$\frac{d}{dx}\left(\rho u \left(h + \frac{u^2}{2}\right) + \tau u - q\right) = 0, \tag{42}$$

$$\frac{d}{dx}(\rho Y_i u + j_i) = 0, \tag{43}$$

$$q = -k\frac{dT}{dx} + \sum_{i=1}^{2} j_i h_i, \tag{44}$$

$$j_i = -\rho \mathcal{D}\frac{dY_i}{dx}, \tag{45}$$

$$\tau = \frac{4}{3}\mu\frac{du}{dx}, \tag{46}$$

$$c_p = Y_a c_{pa} + Y_b c_{pb}, \qquad h = h_o + c_p T, \tag{47}$$

$$c_v = Y_a c_{va} + Y_b c_{vb}, \qquad e = e_o + c_v T, \tag{48}$$

$$p = \rho R T \tag{49}$$

3.3.1 Phase Plane Nodes

The first step in solving the inert shock wave structure was calculating the boundary conditions. By simplifying the governing equations, a system of two ordinary differential equations can be used to create a phase plane. This phase plane has its equilibrium points at the at the boundary conditions for the shock wave. Therefore, the properties of the shock as $x \to -\infty$ and $x \to \infty$ can be solved algebraically. Starting with linear momenta, Eq. (41) the first differential equation can be solved for du/dx

$$\rho u \frac{du}{dx} + \frac{d}{dx}(p - \tau) = 0, \tag{50}$$

$$\frac{d}{dx}\left(\rho u^2 + p - \tau\right) = 0. \tag{51}$$

After applying the product rule, the conservative form of the linear momenta equation remains. τ can then be substituted into the equation to achieve:

$$\frac{d}{dx}\left(\rho u^2 + p - \frac{4}{3}\mu\frac{du}{dx}\right) = 0. \tag{52}$$

Once in the conservative form, the differential equation can be integrated and the boundary conditions can be applied as $x \to \infty$: which yields

$$\rho_1 u_1^2 + p_2 - \underbrace{\frac{4}{3}\mu\frac{du}{dx}}_{=0} = C_1, \tag{53}$$

$$\frac{d}{dx}\left(\rho u^2 + p - \frac{4}{3}\mu\frac{du}{dx}\right) = \rho_1 u_1^2 + p_2. \tag{54}$$

After slight algebraic rearranging, Eq. (54) becomes:

$$\frac{du}{dx} = \frac{3}{4\mu}\left(\rho_1 u_1^2 + p_2 - \left(\rho u^2 + p\right)\right). \tag{55}$$

For the second differential equation, the temperature gradient will be calculated from the heat flux. Starting with the energy and heat flux equations:

$$\frac{d}{dx}\left(\rho u \left(h + \frac{u^2}{2}\right) + \tau u + k\frac{dT}{dx}\right) = 0. \tag{56}$$

At this stage, we can integrate the differential equation and apply the boundary conditions as $x \to \infty$,

$$\left(\rho_1 u_1 \left(h_2 + \frac{u_1^2}{2} \right) + \underbrace{\tau_2}_{=0} u_1 + \underbrace{k \frac{dT}{dx}}_{=0} \right) = C_2 \tag{57}$$

Here τ_2 is the shear stress in the far field which is zero. Using the boundary conditions set from the linear momenta equation in Eq. (54), τ can be solved in terms of the pressure, density and velocity,

$$\tau = \rho u^2 + p - \left(\rho_1 u_1^2 + p_2 \right) \tag{58}$$

Eq. (57) and Eq. (58) can be combined to create the final differential equation needed to describe the phase plane. The set of differential equations used to describe the phase plane are below,

$$\frac{du}{dx} = \frac{3}{4\mu} \left(\rho_1 u_1^2 + p_2 - \left(\rho u^2 + p \right) \right), \tag{59}$$

$$\frac{dT}{dx} = \frac{\rho_1 u_1 \left(h_1 + u_1^2/2 \right) - \rho u \left(h + u^2/2 \right) + \left(\rho_1 u_1^2 + p_1 - \left(\rho u^2 + p \right) \right) u}{k}. \tag{60}$$

The method to determine the stability nodes is outlined by Goodwine [12]. To calculate the different stability nodes of the shock system, Eq. (59) and Eq. (60) were algebraically set to zero to solve all equilibrium points. Once the stability nodes are found, the eigenvalues are used to determine the stability around each equilibrium point. The post-shock equilibrium is a saddle point node, due to the eigenvalues of the differential equations being both positive and negative. Whereas, the pre-shock equilibrium node is a sink stability point; meaning that both eigenvalues were negative. Using this method, Figure 4 was created to show the direction of the phase equilibrium.
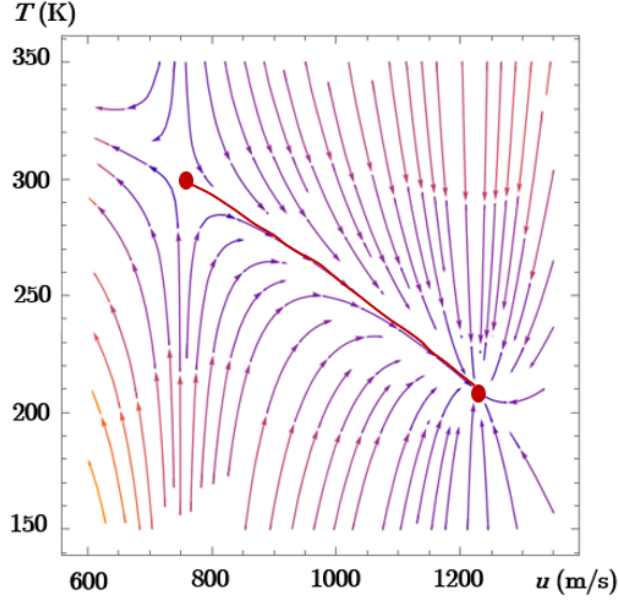
Figure 4: Phase plane of shock with equilibrium points.

The phase plane nodes were then tabulated in Table 3.

Table 3: Boundary conditions of shock properties

Equilibria	Variable	Value	Units
pre-shock	u	1226.017	m/s
	T	209.44	K
	ρ	0.0988	kg/m^3
	p	43.0	kPa
post-shock	u	750	m/s
	T	300	K
	ρ	0.1615	kg/m^3
	p	100.6	kPa

3.3.2   Shock Structure

The viscous shock analysis by Powers [13] to include mixture properties acts as the baseline analysis for a viscous shock wave. The study was then modified to include the mass diffusion analysis. First, we will simplify the governing equation by establishing constraints.

$$j_a + j_b = 0, \tag{61}$$

19

Eq. (61) imposes that the total diffusive mass flux of the system is zero. This restriction allows the heat flux to be simplified to:

$$q = -k\frac{dT}{dx} + j_a h_a + j_b h_b, \tag{62}$$

$$= -k\frac{dT}{dx} + j_a h_a - j_a h_b, \tag{63}$$

$$= -k\frac{dT}{dx} + j_a(h_a - h_b), \tag{64}$$

$$= -k\frac{dT}{dx} \tag{65}$$

Furthermore, because both species a and species b are helium, they have the same specific heats,

$$c_{pa} = c_{pb} \tag{66}$$

The specific heat of the mixture can also be simplified similarly. The mixture c_p can be written,

$$c_p = Y_a c_{pa} + Y_b c_{pb} \tag{67}$$

$$c_p = Y_a c_{pa} + Y_b c_{pa} \tag{68}$$

$$c_p = c_{pa} \underbrace{(Y_a + Y_b)}_{=1} \tag{69}$$

$$c_p = c_{pa} \tag{70}$$

The same analysis is true with specific heat at constant volume. With these assumptions, Eq. (46) and Eq. (65) can be substituted into Eq. (42) to get a new form of the energy equation:

$$\frac{d}{dx}\left(\rho u\left(h + \frac{u^2}{2}\right) + \frac{4}{3}\mu\frac{du}{dx}u + k\frac{dT}{dx}\right) = 0. \tag{71}$$

The thermal conductivity, k, can then be rewritten in terms of the mixture specific heat

and Prandtl number, Pr, then inserted into the energy equation.

$$k = \frac{\mu c_p}{\text{Pr}}, \tag{72}$$

$$\frac{d}{dx}\left(\rho u \left(h + \frac{u^2}{2}\right) + \frac{4}{3}\mu \frac{du}{dx} u + \frac{\mu c_p}{\text{Pr}} \frac{dT}{dx}\right) = 0. \tag{73}$$

Substituting Eq. (47) into (73), the temperature can be rewritten in terms of both static and stagnation enthalpies.

$$\frac{d}{dx}\left(\rho u \left(h + \frac{u^2}{2}\right) + \frac{4}{3}\mu \frac{d}{dx}\left(\frac{u^2}{2}\right) + \frac{\mu c_p}{\text{Pr}} \frac{d}{dx}\left(\frac{h - h_o}{c_p}\right)\right) = 0. \tag{74}$$

Further simplifying the derivative of the constant, $-h_o/c_p$ which equals zero;

$$\frac{d}{dx}\left(\rho u \left(h + \frac{u^2}{2}\right) + \frac{4}{3}\mu \frac{d}{dx}\left(\frac{u^2}{2}\right) + \frac{\mu}{\text{Pr}} \frac{dh}{dx}\right) = 0. \tag{75}$$

Taking Pr to be 3/4, we can further integrate and apply the boundary condition as $x \to -\infty$.

$$\rho u \left(h + \frac{u^2}{2}\right) + \frac{4}{3}\mu \frac{d}{dx}\left(h + \frac{u^2}{2}\right) = C_1. \tag{76}$$

Eq. (76) is a first order ordinary differential equation with the solution:

$$h + \frac{u^2}{2} = \frac{C_1}{\rho_1 u_1} + C_2 \exp\left(-\frac{3\rho_1 u_1 x}{4\mu}\right). \tag{77}$$

Applying boundary conditions, to suppress infinite growth as $x \to -\infty$, C_2 must equal 0. Furthermore, C_1 can be expressed as the following:

$$C_1 = \rho_1 u_1 \left(h_1 + \frac{u_1^2}{2}\right). \tag{78}$$

Substituting these constants into Eq. (77) yields;

$$h + \frac{u^2}{2} = h_1 + \frac{u_1^2}{2}. \tag{79}$$

Applying the caloric equation of state Eq. (49)

$$c_p T + \frac{u^2}{2} = c_p T_1 + \frac{u_1^2}{2}, \tag{80}$$

$$T = T_1 + \frac{u_1^2 - u^2}{2c_p}. \tag{81}$$

The linear momentum equation, Eq. (41), can be rewritten:

$$\rho_1 u_1 \frac{du}{dx} + \frac{d}{dx}\left(p - \frac{4}{3}\mu \frac{du}{dx}\right) = 0. \tag{82}$$

Integrating and applying the mass conservation equation, applying boundary as $x \to -\infty$;

$$\rho_1 u_1^2 + p_1 = C_1. \tag{83}$$

Then apply ideal gas law, Eq. (49), along with Eq. (81) to arrive at

$$\rho_1 u_1 u \underbrace{\underbrace{\left(\frac{\rho_1 u_1}{u}\right)}_{=\rho} R \underbrace{\left(T_1 + \frac{u_1^2 - u^2}{2c_p}\right)}_{=T}}_{=p} - \frac{4}{3}\mu\frac{du}{dx} = \rho_1 u_1^2 + \underbrace{\rho_1 R T_1}_{=p_1}. \tag{84}$$

This differential equation can be simplified to:

$$\frac{du}{dx} = \frac{-\rho_1 u_1^2 - \rho_1 R T_1 + \frac{\rho_1 u_1}{u}\left(u^2 + R\left(T_1 + \frac{u_1^2 - u^2}{2(\gamma-1)/(\gamma R)}\right)\right)}{\frac{4}{3}\mu}. \tag{85}$$

Using the equilibrium points from Subsection 3.3.1, the solution could be numerically integrated from the post-shock to the pre-shock state. The shock had to be integrated in this direction due to the equilibrium stability. The shock is then modeled below in Figure 5 through the: speed, temperature, density, and Mach number.

(a) fluid speed

(b) fluid temperature
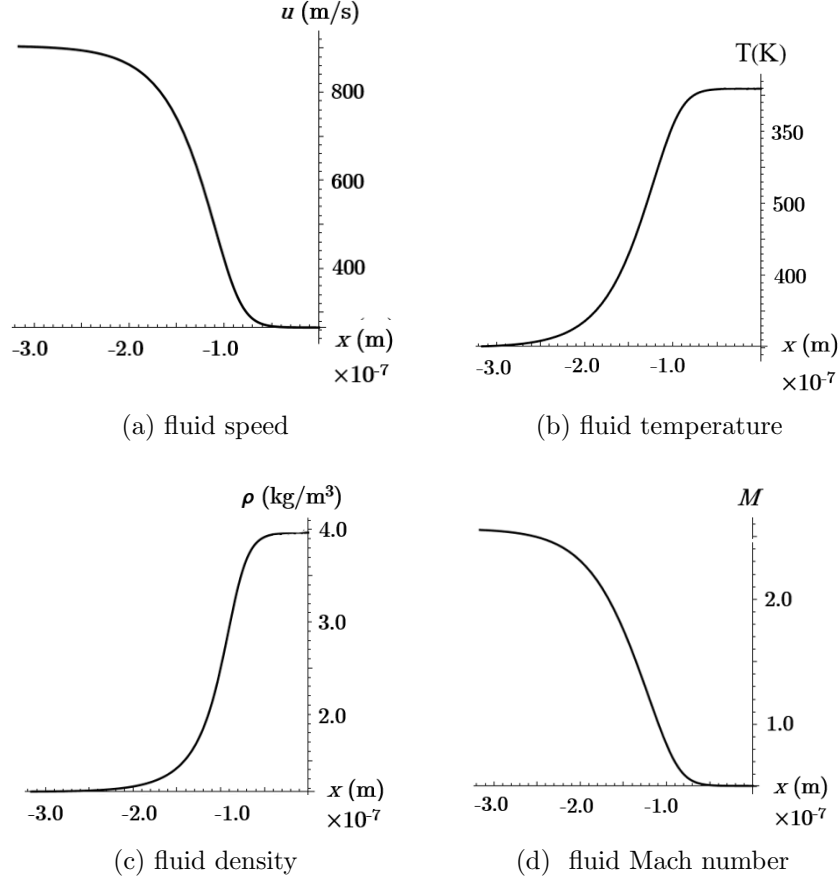
(c) fluid density

(d) fluid Mach number

Figure 5: Viscous shock structure of helium for various thermodynamic properties.

The thickness of the shock wave can be refined using an approximation of the mean free path.

$$\lambda \approx \frac{7.8895 \times 10^{-8}}{\rho} \, [\text{m}]. \tag{86}$$

Here λ is the mean free path between particles in a fluid. The shock thickness is then estimated using the following formula:

$$l_{shock} \approx \frac{8\gamma\mu}{3(\gamma+1)\rho_1(u_1 - u_2)}. \tag{87}$$

l_{shock} is the length of the shockwave and the rest of the parameters are known. Substituting in the known parameters the length of the shock is determined to be 1.3126×10^{-4} mm.

3.3.3 Mass Diffusion Across Shock

To analyze the mass diffusion across the shock, the solution of Eq. (43) must be found. For the mass diffusion analysis, we will define the boundary conditions as such:

Table 4: Boundary conditions for mass red-blue helium mass diffusion

Property	Parameter	Value	Units
x	x_1	$-\infty$	m
u	u_1	1226.017	m/s
ρ	ρ_1	1.615	kg/m^3
j_a	j_{a_1}	0	kg/m^2/s
Y_a	Y_{a_1}	0	

Once the boundary conditions are established Eq. (43) can be integrated.

$$\rho_1 u_1 Y_a + j_a = C_1 \tag{88}$$

At $x \to -\infty$, Y_a and j_a equal zero, which means $C_1 = 0$. In combination with Fick's law in Eq. (45) the species equation becomes,

$$\rho_1 u_1 Y_a - \rho \mathcal{D} \frac{dY_a}{dx} = 0. \tag{89}$$

For this analysis mass and momentum diffusion are assumed to be equal, therefore:

$$\mathcal{D} = \frac{\mu}{\rho}. \tag{90}$$

Further simplifying Eq. (89) into

$$\rho_1 u_1 Y_a - \frac{dY_a}{dx} = 0, \tag{91}$$

$$\frac{dY_a}{dx} = \frac{\rho_1 u_1 Y_a}{\mu}. \tag{92}$$

We can take $Y_a(0) = 1$ to get,

$$Y_a(x) = \exp\left(\frac{\rho_1 u_1}{\mu} x\right).\tag{93}$$

Finally, the mass fraction of species a can be plotted across the boundary. Eq. (6) shows the mass diffusion across the shock boundary. Eqs. $(40 - 93)$ describes the thermodynamics and dynamics across the shock structure in one simplified differential equation. However, to describe the equilibrium of the model in a phase plane, it is necessary to come up with a set of two differential equations.

Utilizing the same numerical integration methods as for the shock structure, the mass diffusion can be calculated. The mass diffusion due to the shock as outlined in Section 3.3, can be found in Figure 6 below:
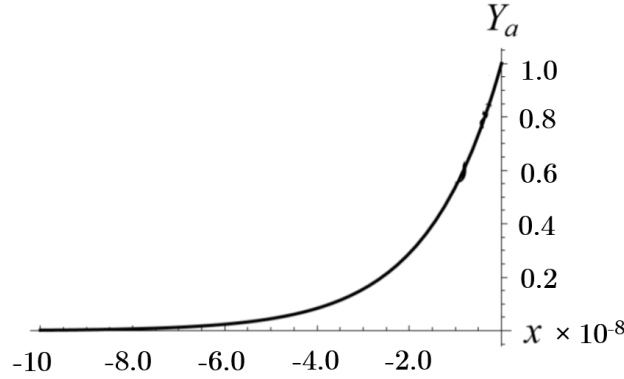

Figure 6: Mass fraction of species a across the boundary with no reaction.

4   Discussion

4.1   Phase Plane Nodes

The vector field created by the phase equilibrium in Figure 4 shows the two equilibrium points in the shock system: the pre-shock and post-shock state. The pre-shock equilibrium point is the sink point, where the velocity, $u = 1226.017$ m/s, and the temperature, $T = 209.44$ K.

To integrate from the sink to the saddle point, the post-shock solution, the initial condition needs to be set off the saddle point then integrated along the solution trajectory towards the sink point. This method integrates from the post-shock solution to the pre-shock solution; however, due to the stability of the pre-shock equilibria, integration from that state to the final stage is impractical. The phase plane is necessary to understand the stability of the equilibrium points and is utilized in the direction of the integration. This is why all solution results are plotted with $x < 0$. For the dissociation problem, the system of differential equations may end up being a phase plane or even a phase volume depending on the .

4.2   Shock Structure

Figure 5 illustrates the shock structure given across the variable thermodynamic properties. As fluid particles hit the shock, the speed and Mach number decrease rapidly across the shock thickness of around 1.3126×10^{-4} mm. Temperature and density of the fluid experience the opposite effect, greatly increasing throughout the shock thickness.

4.3   Mass Diffusion

Figure 6 shows the mass diffusion of the fluid particles across the shock. For the pre-shock solution, the mass fraction of species a was zero, and fully diffused by the post-shock state. This phenomenon is consistent with the boundary conditions established with the mass diffusion and reaffirms the shock thickness of 1.3126×10^{-4} mm.

5   Conclusion

The structure of a viscous shock was determined using purely analytical methods. Utilizing the governing conservation equations, a single ordinary differential equation was solved to find the post-shock solution. Solving for the shock solution via the conservation equations enforces continuity across the shock wave. This allows for the determination of the shock

due to viscosity effects. The shock was then found to be 1.3126×10^{-4} mm thick. Finally, the structure found is consistent with experiments and other theories on the subject.

6   References

[1] Vincenti, W. G. and Kruger, C. H., *Introduction to Physical Gas Dynamics*, Krieger Publishing Company, 1965.

[2] Liepmann, H. W. and Roshko, A., *Elements of Gasdynamics*, John Wiley & Sons, New York, 1957.

[3] Zel'dolvich, Y. B. and Raizer, Y. P., *Physics of Shock Waves and High Temperature Hydronamic Pheonomena*, Dover Publications, Mineola, New York, 2002.

[4] Talbot, L. and Sherman, F. S., "Structure of Shock Waves in a Monatomic Gas," Tech. Rep. 12-14-58W, NASA, 1959.

[5] Thompson, P. A., *Compressible Fluid Dynamics*, McGraw Hill, New York, 1972.

[6] Shapiro, A. H., *The Dynamics and Thermodynamics of Compressible Fluid Flow*, John Wiley & Sons, New York, 1976.

[7] Shapiro, A. H. and Kline, S. L., "On the Thickness of Normal Shock Waves in a Perfect Gas," *Journal of Applied Mathematics*, Vol. 2, 1955, pp. 185–192.

[8] Sherman, F. S., "A Low-density Wind-tunnel Study of Shock-Wave Structure and Relaxation Phenomena in Gases," Tech. Rep. 3298, NACA, 1955.

[9] Borgnakke, C. and Sonntag, R. E., *Fundamentals of Thermodynamics*, Wiley, 9th ed., 2017.

[10] Powers, J. M., *Combustion Thermodynamics and Dynamics*, Cambridge University Press, 2016.

[11] Bird, R. B., Stewart, W. E., and Lightfoot, E. N., *Transport Phenomena*, John Wiley & Sons, New York, 2002.

[12] Goodwine, B., *Engineering Differential Equations Theory and Applications*, Springer, 2011.

[13] Powers, J. M., *Mechanics of Fluids*, Cambridge: Cambridge University Press, 2024.